Front. Comput. Sci., 2019, 13(1): 170–182
https://doi.org/10.1007/s11704-016-6191-1

RESEARCH ARTICLE

A fast registration algorithm of rock point cloud based on spherical projection and feature extraction

Yaru XIAN, Jun XIAO (✉), Ying WANG

School of Artificial Intelligence, University of Chinese Academy of Sciences, Beijing 100049, China

Abstract Point cloud registration is an essential step in the process of 3D reconstruction. In this paper, a fast registration algorithm of rock mass point cloud is proposed based on the improved iterative closest point (ICP) algorithm. In our proposed algorithm, the point cloud data of single station scanner is transformed into digital images by spherical polar coordinates, then image features are extracted and edge points are removed, the features used in this algorithm is scale-invariant feature transform (SIFT). By analyzing the corresponding relationship between digital images and 3D points, the 3D feature points are extracted, from which we can search for the two-way correspondence as candidates. After the false matches are eliminated by the exhaustive search method based on random sampling, the transformation is computed via the Levenberg-Marquardt-Iterative Closest Point (LM-ICP) algorithm. Experiments on real data of rock mass show that the proposed algorithm has the similar accuracy and better registration efficiency compared with the ICP algorithm and other algorithms.

Keywords rock point cloud, registration, LM-ICP, spherical projection, feature extraction

1 Introduction

In recent years, the rock mass engineering plays a more and more important role in all kinds of infrastructure construction with the development and utilization of natural resources. For the huge scale of jointed rock mass engineering, it is difficult and dangerous to implement, and hard to be recovered once the operational errors occur, so it is difficult to carry out massive repetitive experiments. Recently, the rapid development of 3D laser scanning technology, which can obtain a wide range of spatial 3D data directly by using a non-contact active measurement in a short time [1], makes 3D modeling more convenient and accurate. Meanwhile, 3D laser scanning technology can scan a wide range of objects, and it has the ability to overcome the restriction of traditional measuring method, which is easily affected by natural light. The scanning measurement has many advantages, such as fast speed, real-time performance, high accuracy, strong initiative, high degree of digitalization, and high measuring efficiency. Numerical experiment method, using the surface information of the object obtained by the 3D laser scanner, shows its superiority with the development of computer-aided design technology. The method of computer numerical simulates model for rock mass through the usage of detailed data, and simulates the different conditions, such as geological structures and the surrounding environment by setting complex parameters. Meanwhile, by combining the simulation with computer visualization and 3D animation display, the dynamic scene of the construction field is simulated vividly. From the simulation above, the adequate comparisons are provided on different schemes, and it provides guidance and macro-control to the project.

In 3D laser-scanning device, laser is the basement of the measurement, and the propagation characteristic of light makes that the laser scanning can only collect the information in one direction in a perspective. While there may be occlusion of the view when we capture the surface informa-

Received March 31, 2016; accepted August 25, 2016

E-mail: xiaojun@ucas.ac.cn

tion of the specific object, and the object may be very huge, the geometry of the object or the surrounding environment can be complex. In order to get the complete point cloud data of the object surface, the object should be scanned from a number of different perspectives, and a suitable coordinate system should be given. Because each view has its own coordinate system, the data measured in different views should be transformed into a unified coordinate system. The process above is called registration.

Depending on whether the initial information is required, the registration methods can be divided into two steps: coarse registration and fine registration [2]. Coarse registration generally provides only the approximation of the transformation between two clouds, thus narrowing the gap between the two clouds to improve the efficiency of registration. The fine registration minimizes the gap between the overlapping regions using an iterative method based on an initial estimation, which further improves the accuracy of registration.

The most widely used approach of fine registration is the ICP algorithm proposed by Besl & McKay [3] and Chen & Medioni [4], which optimizes the transformation by an iteration algorithm. For every point in the source cloud, the algorithm searches for the closest point in the target cloud in every iteration, and then calculate the corresponding transformation from their correspondence. Its computational efficiency is low because every point needs to be traversed in the process, especially for large objects such as rock, which has a huge amount of points. Therefore, the speed of convergence in actual operation is of great importance.

It is much earlier and more developed for the research of image registration than point cloud registration in various fields. Comparatively the method of point cloud registration is immature and relatively small. For the environment of rock mass is complex and changeable, which has few features as obvious as artificial architecture, a few mature point cloud registration algorithm can be applied to rock environment. The iteration process of ICP does not require any features, since it can be calculated from the point data directly, so it is of high applicability. Therefore, an improved ICP algorithm will be used in this paper. It is extraordinarily time-consuming since the calculation process of ICP requires iterating through all of the points. To solve this time-consuming problem, we combine the ideas of image registration with ICP. Firstly, we obtain the data similar to the 2D data by projecting all of the 3D points onto the spherical coordinates, and extract feature points from the projected data. The time of extracting feature points will be shortened by reducing data dimensions in this step. Secondly, we choose the good corresponding point-pairs through a series of optimization algorithms. Finally, we carry out the subsequent iterative calculations with the point-pairs obtained in the last step. Since the number of points we used is far less than the original data, the time used in every iteration is greatly reduced, and the number of iterations is reduced too, because the point pairs are almost matching.

2 Related work

2.1 Coarse registration

The registration based on the measurement device is the easiest method of coarse registration. General data collection devices can record the scanning position and angle, so we can read the conversion information from the scanning devices directly, and use it as the initial estimation. The method relies on the accuracy of the scanning device, but the higher the precision of the device is, the more expensive the price will be. Besides, devices need to be adjusted in practice and the more sophisticated the instruments are, the more complex the adjustment process will be. The adjustment process of the device has a great influence on the measurement results.

The method of setting fixed targets in the scene is the most direct method of coarse registration [5]. The targets are generally divided into two types: 2D planar target and 3D target. The 3D target is generally spherical, so once found, it is easy to calculate its central location. Because of its consistency of projections in all directions, 3D target is widely used. The paper [6] points out the method of setting fixed targets is also called semiautomatic registration method. A traversing data registration method was proposed and compared with common point data registration method and the orientation data registration method [7].

Most commercial scanners like to use 3D targets to match different scenes. This method requires the presence of at least three non-collinear targets in public areas of the scene to be registered, and determines the coordinates of the center of each target within its own coordinate system after the point cloud information of these scenes was captured, from which we can calculate the transformation. However, this method has many limitations. For example, the rock environment searched in this paper is complex, therefore there may be not appropriate locations to lay the targets.

The method of interactively selecting corresponding points is similar to the method of setting fixed targets. In this method, we compute the transformation from the manually selected matching points. If the obtained data is good and shown in a high recognizable degree, we can get a good registration result even under such conditions that overlapping areas are small or initial positions are bad. However, if the data have such a low resolution that the objects are not recognizable, it will be very difficult to extract the matching positions, thus affects the registration accuracy.

Most of the aforementioned methods of coarse registration are based on certain geometric features of the objects. Such as the classic Point Signature-based [8] method and Spin Image-based [9] method, the disadvantage of these methods is heavy calculation burden, so they are not suitable for cases in which data are massive. Later, methods based on linear segments [10, 11] are proposed. These methods can produce good results in objects with obvious linear features such as buildings, but not for complex objects with curves and surfaces. There are also some other methods of coarse registration, such as the method based on the joint of principal directions [12] and the method of Euclid invariant features based on integration [13–15], both of which have high robustness for noise. Besides, there are some methods based on the high-level features such as the similar invariance of point or line [16]. More details about coarse registration can be seen in [17].

2.2 Fine registration

ICP is the most widely used method of fine registration. The corresponding points between two clouds are found in this method, from which the transformation will be estimated. The matrix will be applied to the source to form a new source, and set the new source to be the source in the next iteration. Through the iterations, we can gradually reduce the gap between the source and the target, until it reaches a predetermined threshold value. Finally, we obtain the overall transformation matrix. Since the algorithm must traverse all of the points, the calculation is slow for huge amount of data. What's more, the algorithm requires the clouds to be in good initial positions, so generally it is only used as the fine registration. In addition, if there is no sufficient overlap between the inputs, the registration cannot be completed successfully.

There are many improved algorithms proposed for the problems of ICP. Most of the proposed algorithms are from several aspects, such as changing the search strategy, eliminating noise effects, and removing the bad corresponding points. For example, the Hong-Tan based ICP (HT-ICP) [18] algorithm uses a distance between a point in the source and the projection in the target rather than the closest point to eliminate the mismatched points effectively. A method removing noise by using the Euclidean distance is proposed by Zhong and Zhang [19]. The method improved the ICP by setting a threshold of the angle between the direction vectors of the source and the target. There are also a number of other algorithms improve ICP from these aspects [20, 21]. The LM-ICP [22] algorithm uses a nonlinear minimization optimization to eliminate mismatching, which can minimize the energy function directly. The method improves the robustness and convergence speed of ICP significantly without increasing time-consuming.

In addition, the Normal Distribution Transform (NDT) [23] algorithm is proposed as a method of fine registration based on statistical information. The original method was applied to 2D space. The spatial scanning position is subdivided into unit squares, and then the method calculates the probability distribution of each square using the distribution of the points in the squares. The 3D form of the method [24] is based on the cell cubes, and optimizes the results by using standard optimization techniques. NDT method calculates through the statistical information rather than every point, and it improves the efficiency of registration greatly compared with the ICP algorithm.

2.3 The registration based on image

The research of image registration is much earlier and more developed than that of point cloud registration. Many scholars combine image registration with the registration of point cloud. Nowadays many 3D scanners are equipped with high-precision cameras, thus an image of the object can be achieved while the 3D point cloud is obtained. Then we can register the points with the assistance of the corresponding 2D images. For example, Yang et al. [25] match the camera image with the image generated from scanner by a scale invariant transformation characteristics, thus to register the 3D data by registering the images. Moreover, in some papers such as [26, 27], they register by using the scanner data and the camera assembled on the scanner. In addition, there are some other methods register the point cloud data combined with range images [28].

2.4 Feature extraction

During the development of computer vision, the process of extracting the key pixels of the image, describing the image with neighborhood information of the key pixels, analyzing the pixels and determining the characteristics attributable in order for the computer to recognize the image is called feature extraction.

There should be some differences such as translation, rotation, scaling and even illumination, occlusion among the images taken at different angles of views for the same object. To study the characteristics is to study the invariances that exist under these changes, to reflect the basic attributes of the images, to distinguish the color or texture information from different images. Good characteristics should not only have the invariance to these changes, but also have reliability and independence. There are varieties of characteristics applied in the field of computer vision currently, and it is hard to say which one is better, for their applications are different depending on the conditions.

The features mostly used include point feature, line feature, and some high-dimensional features, etc. One of the most typical features is SIFT [29] algorithm, which has certain invariance of light, geometrical transformation, rotation and so on. Then someone proposed some point features such as the acceleration characteristic named Speed-up Robust Features (SURF) [30] and Oriented Fast and Rotated Brief (Oriented Brief, ORB) [31, 32] algorithm aiming at the problem of computationally intensive of the SIFT algorithm. There are also some new local features can be used for registration, such as the local feature statistics histogram(LFSH) [33] and so on. Most of the high-dimensional features, which are explored and researched based on the original simple features narrow the applicable scope because of their complexity, and are more time-consuming.

3 Proposed method

3.1 Basic framework

The process of the fast registration algorithm based on spherical coordinate projection is shown in Fig. 1. Firstly, we need data preprocessing before registration so that the data can be applied to the Point Cloud Library (PCL) easily for convenient reading and writing, and supports user-defined data structure. Therefore, the format should be converted into the PCD file before loading it. The point cloud that is organized or unorganized will be treated differently in this paper when converted to a 2D image. The disadvantages brought by the different resolutions and different angles of views when searching for the correspondence between the camera image and the point cloud is avoided with respect to the method that registers the point clouds through registration of the image captured by precision camera assembled on the scanner. Then we extract features in the 2D image, select features that can be well matched, and remove the mismatching points. After that, the sub-clouds can be obtained by sampling the original data according to the remaining pixels. Finally, the transformation is obtained by the LM-ICP algorithm, which will be applied to the source. The source and the target will be unified into the same coordinate system through an iterative process, then the Euclidean fitness score of the registration result will be calculated.

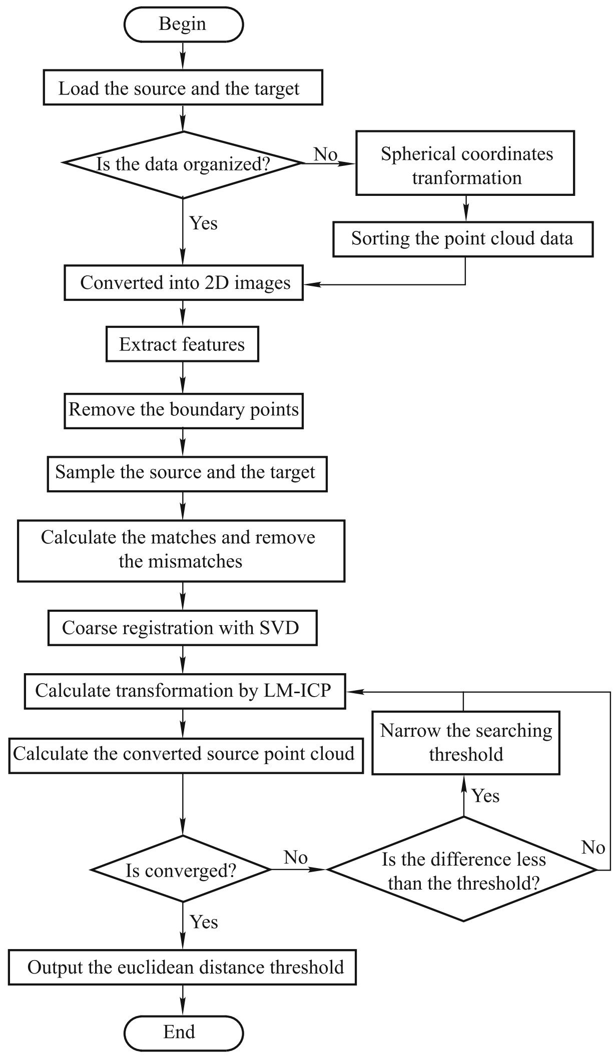

Fig. 1 Algorithm progress

3.2 Image projection transformation

The acquired point cloud data can be divided into organized point cloud dataset and unorganized point cloud dataset, and the data in different forms should be treated differently in this paper. There are two parameters named WIDTH and HEIGHT in the PCD files, which tells us whether the data is organized by indicating the width and height of the point cloud dataset. The parameters HEIGHT and WIDTH represent the number of rows and the number of points in each line in the file respectively in the organized point cloud, but the HEIGHT will be set to be one and the WIDTH can show the number of points in the cloud in the unorganized point cloud. Therefore, we can know whether it is organized by the parameter HEIGHT after loading the data.

The organized data used in this paper are obtained from the Kinect. The data are split into rows and columns resembling a matrix or an image. Thus, we can know the relationship between adjacent points by the indices of the points and the adjacent-domain operation will be much convenient and efficient, and the computing speed will be accelerated. An image can be generated directly by the correspondence between the indices of the points and the position of the pixel, then form a match of point-to-point between the point cloud and the image, causing neither the loss of information in the point cloud, nor the missing of pixels in the image.

However, there are no such relationships for the unorganized point cloud, so there must be some calculating operations before they can be converted into images. We will introduce the conversion methods in next part.

3.2.1 Transformation principle

The working principle of the ground pulse 3D laser scanner is shown in Fig. 2. The scanner emits pulse laser to the object surface, each scan line intersects with the spherical centered at the scanner at a unique point, and the intersections do not coincidence with each other. The method of obtaining the data of the scanner is divided into horizontal scan and vertical scan, the points in the horizontal scan lines have the same vertical angle ψ and the vertical ones have the same horizontal angle θ. Since the intersections of each line with the spherical are unique and do not coincide, the original data can be mapped to the spherical polar coordinate system uniquely from the 3D cartesian coordinate system using the relationship between the spherical coordinate system and cartesian coordinate system. Then convert the points to a standard 2D image according to the horizontal angle and the vertical angle.

The spherical coordinate system is shown in Fig. 3. Assume that the point $P(x, y, z)$ is a point in the space, then the point can also be presented by three ordered numbers (r, θ, ψ) in the spherical coordinate system, wherein r presents the distance between the origin O and the point P, ψ is the angle between the directed line segment OP and the positive Z-axis. The point M is the projection of the point P projected to the plane XOY, θ is the counterclockwise rotation angle from the X-axis to OM view from the positive Z-axis. Such a set of numbers r, θ, ψ is called the spherical coordinate of the point P, the variation ranges of parameters r, θ and ψ are $r \in [0, +\infty)$, $\theta \in [0, 2\pi)$ and $\psi \in [0, \pi)$ respectively.

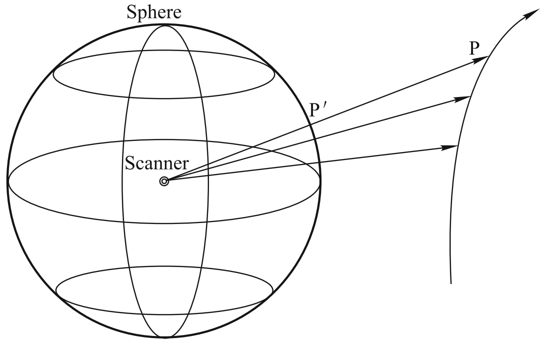

Fig. 2 The working schematic diagram of single station scanner

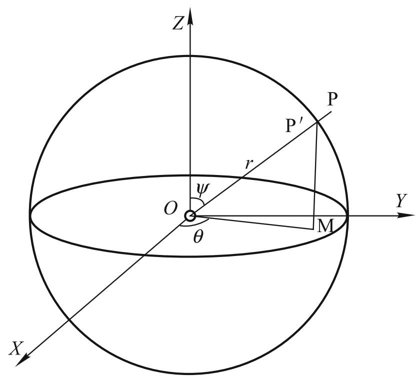

Fig. 3 The spherical coordinate frame

The conversion relationship between cartesian coordinate system and spherical coordinate system is:

$$\begin{cases} r = \sqrt{x^2 + y^2 + z^2}, \\ \psi = \arccos \dfrac{z}{r}, \\ \theta = \arctan \dfrac{y}{x}. \end{cases} \tag{1}$$

3.2.2 Transformation steps

The method of converting a set of unorganized point cloud to an image is as follows:

1) Traverse all of the points and calculate the angle of each point in the spherical coordinate;

2) Calculate the minimum and the maximum of the horizontal angle, determine the angular resolution according to the angle range, then do the same to the vertical angle;

3) Calculate the row and column value of each point according to the angular resolution, which can determine the corresponding pixel location in the image of the point;

4) Define an image according to the ranks, of which the

height is the maximum number of the row and the width is the maximum number of the column. Then calculate the distance between the pixel location of one point and the center of the corresponding pixel, then sort the points in a cloud according to the principle of row column, and the principle becomes the distance between pixel center and the projection from near to far while there are points of equal row and equal column.

We can set the exact resolution of the conversion in the case that we knew the scanner resolution beforehand to avoid overlap or empty, while the cloud data used in this paper are not acquired with a scanner by us, so we do not know the exact resolution of the scanner and we must try to define it. Even though it may not be correct and cause some overlaps or blanks, the data are not exactly scanner data but photogrammetric, so the resolution should not be too high otherwise there may produce many blanks. The transformation result can be seen in Fig. 4.

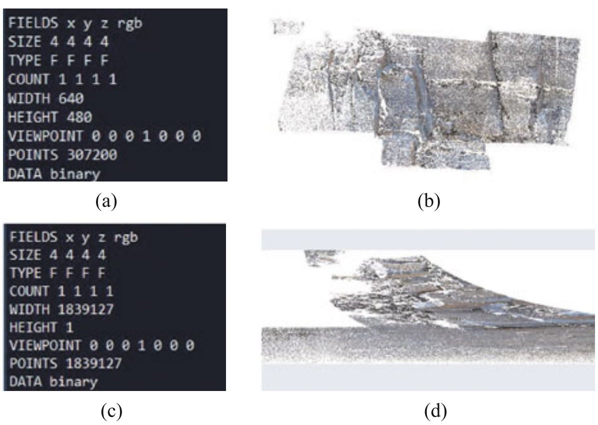

Fig. 4 Transformation result. (a) Information of organized point cloud; (b) image of organized point cloud; (c) information of unorganized point cloud; (d) image of unorganized point cloud

3.3 Feature selection

3.3.1 Extract feature

Local feature structural characteristic describes the invariance of light and geometric transformation using the local information of the local structure in the image. Since the local feature does not depend on the results of image segmentation, thus has a good robustness for occlusion, overlapping and so on [34]. Point feature is one of the most common local characteristics, and also the simplest feature. Although there are also line features, region features and higher dimensional features, there is no such a feature that is unique and ubiquitous in rock mass due to the complexity of the rock mass environment, so the complex features are not applicable in all rock mass, and the more complex the features are, the higher the computation cost is. Therefore, this paper chooses the simplest features. After comparing a few common and typical point features from the principle and experiments, we choose a feature that costs shorter time and has the best result in the comparison, SIFT, which can handle the translation, rotation and affine transformation between images well.

Since the coordinates of the extracted points are mostly not integers, they cannot correspond to the row and column value directly in the progress of corresponding the feature pixels to the original point cloud. We correspond the four nearest points to that point for subsequent calculation.

For organized point cloud, we find the 3D corresponding point by the relationship between the coordinates of feature points and the indices of the original cloud. Nevertheless, for unorganized point cloud, we should sort the extracted feature pixels according to the row column, the same for the corresponding original data, then we can find the corresponding points in one traversal only, through which we can greatly reduce the time required to find the points.

3.3.2 Remove the boundary point

First of all, we introduce a Gaussian template to blur the image in the process of feature extraction, which results in a lack of edge of the image, therefore the features detected at the boundary of the image may not be accurate, and we remove the ones at the boundary first to avoid the impact of the bad features.

Secondly, since the improper selection of the resolution or the precision of the scanner settings, it may lead to blanks in the image generated from the unorganized point cloud. We set the image background to be white therefore, in order to determine whether the extracted feature points is a boundary point within the image, the white points that are not the background in the image are replaced by the color very close to white, so that we can remove the inner edge points by testing the white points.

3.4 Selection of matching

The features extracted by the SIFT algorithm may have many false matches for some partially overlapping data, thus we need to detect the matching relationship of the features to reduce the impact on the result of the false match. The match selection will be done after the pixels converted back to the point cloud in order to reduce the influence to the data accuracy during the conversion process.

The corresponding estimation is produced by the function "determineReciprocalCorrespondences" in PCL, in which only the overlapping portions of the clouds are used to search the corresponding point of each point in the source in the target, and vice versa. The point pair will be set as the corresponding points only if they can form a two-way corresponding.

The un-corresponding removal is produced through the RANSAC-based data-aligned rigidity-constrained exhaustive search (RANSAC-based DARCES) [35] method based on the corresponding relationship calculated in the previous step to solve the set that makes most of the point pairs meet a good match through an iterative sampling process. Select three points in the source randomly firstly, sign them to be the main point p, the second point q and the auxiliary point t respectively, the distances between every two points are d_{pq}, d_{pt} and d_{qt}. The corresponding points in the target of these three points are p', q' and t' respectively, and the distances are d'_{pq}, d'_{pt} and d'_{qt}. We believe these three sets of corresponding relationship are established if the distances match respectively within certain thresholds, through which we can determine the candidate initial transformation. After several iterations, we select the candidate transformations that make most of the corresponding points coincide to be the initial transformation. The algorithm used in this paper is the basic method of random sampling, and there are also many upgrade methods, such as the method proposed in [36].

3.5 Transform

Coarse registration is produced based on the corresponding relationship determined in the prior step firstly. The method of coarse registration used in this paper is the method based on Singular Value Decomposition (SVD), this method constructs adjacent matrix by taking advantage of the information of the distance between the feature points and conduct the SVD of it to obtain the corresponding relationship. Then the fine registration will be done by the LM-ICP algorithm to calculate the transformation matrix using the sub-point cloud obtained by feature extraction.

The ICP algorithm is to register two point sets and minimize the predefined error function by an iteration process. The coordinate transformation is represented by the unit quaternion [37]. Assuming that target point set is P and the reference point set is X, meanwhile the rotation matrix is $R(\overrightarrow{q}_R)$ and the translation vector is $\overrightarrow{q}_T = [q_4 q_5 q_6]^{\mathrm{T}}$, wherein the rotation transformation vector is the unit quaternion $\overrightarrow{q}_R = [q_0 q_1 q_2 q_3]^{\mathrm{T}}$, $q_0 \geqslant 0$, $q_0^2 + q_1^2 + q_2^2 + q_3^2 = 1$ and the letters with "→" on them respect vectors, then the coordinate transformation vector can be expressed completely as $\overrightarrow{q} = [\overrightarrow{q}_R | \overrightarrow{q}_T]^{\mathrm{T}}$. Then the problem of calculating the best coordinate transformation vector of the corresponding sets can be converted into the sake of $\overrightarrow{q}$ to minimize the objective function described in the Eq. (2).

$$f(\overrightarrow{q}) = \frac{1}{N_p} \sum_{i=1}^{N_p} \|\overrightarrow{x}_i - R(\overrightarrow{q}_R)\overrightarrow{p}_i - \overrightarrow{q}_T\|^2. \tag{2}$$

We suppose that the two point sets have already been registered by the coarse registration. Then we should search for the corresponding points in the reference point set for each point in the target point set to construct the corresponding point pairs $(\overrightarrow{p}_i, \overrightarrow{x}_i)$, from which we will perform the following calculations.

Then we find the centers of gravity of the two sets, and use them to construct the covariance matrix shown in the Eq. (3), from which we can construct a 4×4 symmetric matrix shown in the Eq. (4).

$$\sum\nolimits_{PX} = \frac{1}{N} \sum_{i=1}^{N} [\overrightarrow{p}_i \overrightarrow{x}_i^{\mathrm{T}}] - \overrightarrow{\mu}_P \overrightarrow{\mu}_X^{\mathrm{T}}, \tag{3}$$

$$Q\left(\sum\nolimits_{PX}\right) = \begin{bmatrix} tr\left(\sum_{PX}\right) & \Delta^{\mathrm{T}} \\ \Delta & \sum_{PX} + \sum_{PX}^{\mathrm{T}} - tr\left(\sum_{PX}\right) I_3 \end{bmatrix}, \tag{4}$$

where N is the number of the corresponding points, $\overrightarrow{\mu}_P$ and $\overrightarrow{\mu}_X$ are the centers of gravity of the two sets of point respectively, $tr\left(\sum_{PX}\right)$ is the trace of $\sum_{PX}$, $\Delta = [A_{23} A_{31} A_{12}]^{\mathrm{T}}$, $A_{ij} = \left(\sum_{PX} - \sum_{PX}^{\mathrm{T}}\right)_{ij}$ is an anti-symmetric matrix, I_3 is the identity matrix.

Calculating the eigenvalues and eigenvectors of the symmetric matrix Q, then the eigenvector corresponding to the maximum eigenvalue will be selected as the optimal rotation vector $\overrightarrow{q}_R = [q_0 q_1 q_2 q_3]^{\mathrm{T}}$ and the optimal translation vector can be calculated by the formula $\overrightarrow{q}_T = \overrightarrow{\mu}_X - R\left(\overrightarrow{Q}_R\right)\overrightarrow{\mu}_P$ easily.

The transformation matrix calculated in the previous step then be brought to the reference point set, compute and verify whether the minimum mean square error (MMSE) meets the convergence condition, if not, set the transformed reference point set to be the new reference point set in the next iteration. Repeat the above steps until convergence, the final transformation will be the product of the transformations calculated in each iteration.

Each iteration in the ICP algorithm can be summarized in two steps, named the compute correspondence and the update transformation. LM-ICP algorithm optimizes the squared residuals of the ICP algorithm by applying the Levenberg-Marquardt (LM) method, which makes the result more robust and the calculation more quickly.

4 Experimental results and analysis

4.1 Experimental data and evaluation standard

The unorganized point cloud data used in this paper are in granite condition of road cut where the latitude and longitude are 44°24’04.41”N and 76°18’90”W respectively in Kingston, Canada. The data we use is acquired by a Leica HDS6000 whose scan type is phase based from three scan locations in 2007, the point spacing of it is less than 1cm. They come from Rockbench repository [38] which is a web-based common repository for assessing rock mass characteristics using LiDAR and photogrammetry established by Lato contain a number of key items of rock mass. All experiments were carried out by using C++ software combined with PCL that runs on Microsoft Windows 10 Processing, time given below is all counted on a PC, which configuration is Intel (R) Core (TM) i3-2100 3.10 GHz CPU, 6 GB RAM.

The comparative indicators used in the experiments are the following two:

• The time spent by registration The time is computed by the computer automatically and displayed on the screen after the completion of registration.

• The Euclidean fitness score The Euclidean fitness score is the sum of the squared distance of source and the target clouds provided in the PCL. The parameter is a relative parameter that there is no comparability for the feedback results of different sets of data. The quality of the results returned from different methods of the same set of data that have considerable overlap can be judged according to the relative size of the score, the smaller the score, the better the result. However, there is poor applicability of this parameter for the sets with small overlapping regions.

4.2 The influence of resolution

The feasibility of registration using panorama has been proved, so the data of this paper are mainly non-scanning point cloud data. There is a certain uncertainty in the setting of the angle resolution, thus we must try to select it. Besides, the data are not the scanner data, so if the resolution is too high, there will be many blanks in the generated image. Therefore, the resolution should not be too high, though there will be coverage points if the resolution is too low.

Then we explore the registration results of a specific source and a specific target under different resolutions. The information of the two clouds is shown in Table 1, in which the “min” represents the minimum value, the “max” represents the maximum value, the “range” represents the variation range of the angle, the unit of which is degree (“°”), and the data shown in the table are all counted and displayed by computer.

The experimental results are shown in Table 2, in which the “h” in the first column represents “horizontal” and “v” in the second column represents “vertical”. By comparing the registration results of different resolutions we can know that the higher the resolution is, the fewer the points are covered, the more feature points are extracted, and the slower the rate of registration is. There may be some mistakes during extracting feature points at a lower resolution since there are more points covered, resulting in a decreased accuracy of registration. When the resolution comes to an appropriate value, a higher resolution only increases the time the registration cost but decreases the effect, since a high resolution may lead to more blanks in the generated image, which will affect the accuracy of the extracted features. Multi-resolution comparative results are shown in Fig. 5, which shows that there will be a little deviation of registration result when the resolution is relatively low. When the resolution reaches a certain value more appropriate, the changes within a certain range of the resolution will have little effect on the registration results, nevertheless a too high resolution will increase the registration error on the contrary. Therefore, when the exact parameters of laboratory equipment are unknown, we can select a comparatively small value as the appropriate one instead of a higher one.

4.3 Comparison of experimental results

The comparison method used in this paper is the LM-ICP algorithm, the 3D-NDT algorithm and the Sparse Iterative Closest Point(SICP) [39] algorithm.

Table 1 Information of the experimental data

Point cloud	Data size	Horizontal angle			Vertical angle		
		min/°	max/°	range/°	min/°	max/°	range/°
Source	1,600,825	0	360	360	164.515	180	15.4846
Target	1,128,117	0	359.972	359.972	65.2	180	11.5011

Table 2 Experimental results of different angular resolutions

Angle resolution/°		Cloud size		Image size		Number of features		Time/ms	Fitness score
h	v	Source	Target	Source	Target	Source	Target		
0.1	0.1	160,587	169,718	3,603×155	3,600×116	1,596	1,846	2,345	0.231524
0.08	0.08	225,136	240,432	4,504×194	4,500×144	3,290	3,244	2,837	0.226842
0.05	0.05	411,414	453,378	7,204×310	7,200×231	10,258	10,037	5,575	0.22822
0.04	0.04	515,164	580,134	9,004×388	9,000×288	16,236	16,216	6,944	0.255535
0.1	0.01	609,896	710,858	3,604×1,549	3,600×1,151	26,915	27,285	9,371	0.297254

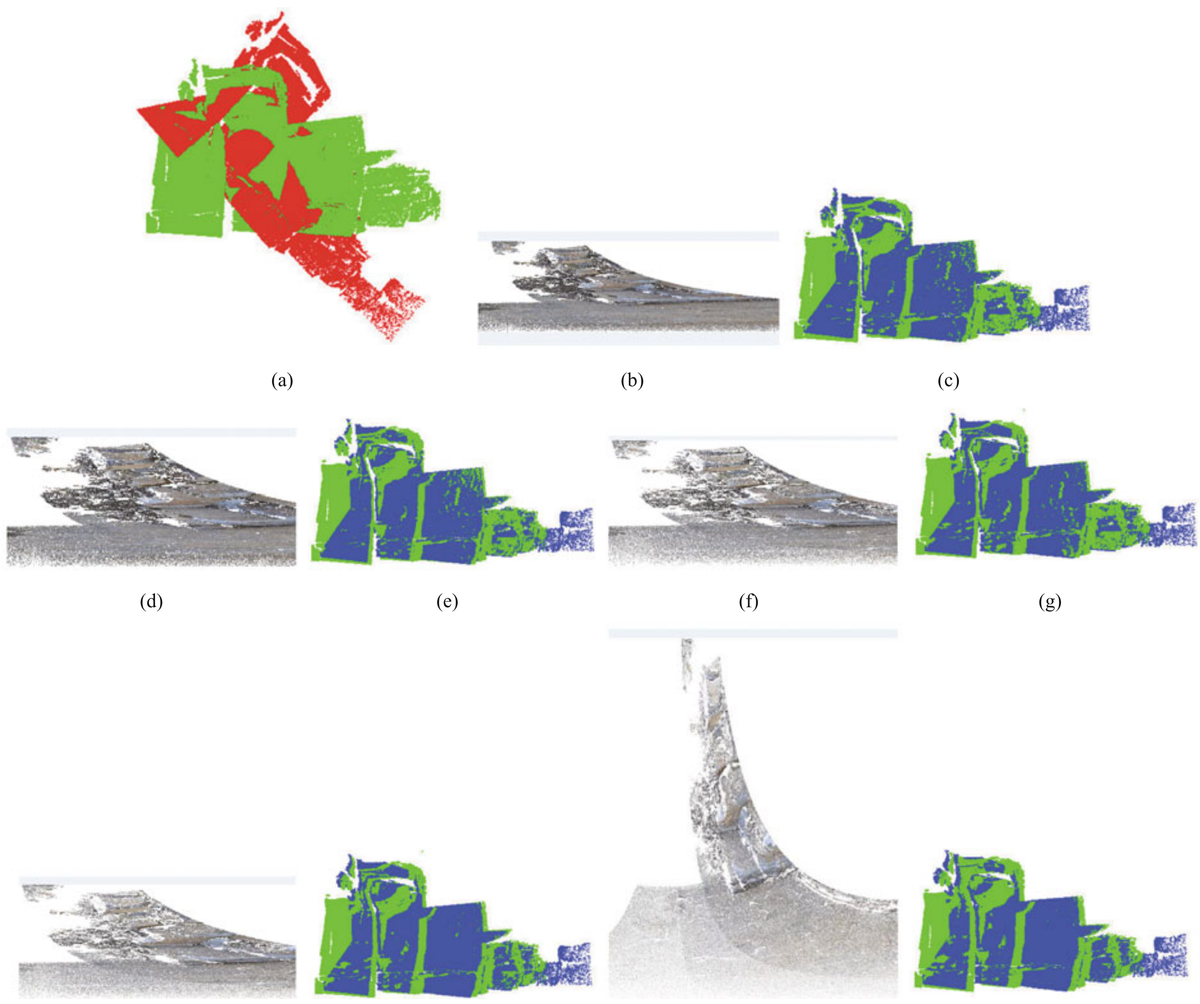

(a) (b) (c) (d) (e) (f) (g) (h) (i) (j) (k)

Fig. 5 Multi-resolution registration results. (a) Point cloud before registration which red points are source and green points are target; (b)–(k) the generated images and registration results of different resolutions in which green points are target and blue points are the registered source (the horizontal resolution × the vertical resolution of the Figs. (b)–(f) are 0.1×0.1, 0.08×0.08, 0.05×0.05, 0.04×0.04 and 0.1×0.01 respectively)

• LM-ICP ICP is the most widely used point cloud registration algorithm, and many algorithms after that are variants of it. Among the variants, LM-ICP minimizes the registration error directly by using a kind of nonlinear optimization, that is, Levenberg-Marquardt algorithm, thus to acquire a comparable speed and more robust result when being compared to ICP.

• NDT NDT uses iterative subdivision to build surface description of models, and avoids the computationally challenging nearest-neighbor search, so NDT is faster and slightly more reliable than ICP in most cases.

• SICP The SICP algorithm implicitly models outliers using sparsity and replaces the Euclidean distance using l_p norm, so that the impact of outliers and incomplete data can be reduced. The use of Lagrange method makes the algorithm more reliable than the heuristic model registration.

Since there is no correlation function of this algorithm in the PCL, the experiments associated with this algorithm in this paper are all based on the code in GitHub and Computer Graphics and Geometry Laboratory, from a certain extent, this will make the run time longer than the PCL functions.

In this paper, LM-ICP is mainly used to be the contrast of registration accuracy, and NDT is mainly the contrast of computational efficiency, the SICP algorithm is used to be a contrast method as a representative of new variation of ICP proposed in resent years. In order to speed up the search process, all of the original point data is used in the proposed algorithm and LM-ICP algorithm, while the filtered data with a voxel filter of the same parameters is used in 3D-NDT, SICP and LM-ICP, and the experiments with the filtered data are all named with "filtered".

The results of registration of organized point clouds are shown in Table 3, the source and target point clouds used in the experiment both contain 307,200 points, and the numbers of the data in the filtered LM-ICP are 1,846 and 1,741 respectively. We can see that the time cost of our proposed method in this paper can achieve about 1/4,600 of the original method, less than 1/460 of the filtered LM-ICP and almost 1/8 of NDT algorithm. In the case of registration precision, the result is better than the filtered LM-ICP, and the disparities from the LM-ICP and NDT are all smaller than 1mm, which is within the precision error of the data. Registration results are shown in Fig. 6, in which green points are points in target cloud, red points are points in source cloud and blue points are points in the transformed source point cloud. It can be seen in the figure that there is almost no difference of the registration results in visualization.

Table 3 Experimental results of organized point cloud

Method	Time/ms	Euclidean fitness score
Proposed method	933	0.00117877
LM-ICP	101,163	0.000994068
Filtered LM-ICP	92,149	0.00117864
Filtered 3D-NDT	2,172	0.001193895
Filtered SICP	693,501	0.0968459

The results of registration of unorganized point clouds are shown in Table 4, the source and target point clouds used in the experiment both contain 1,839,127 points, and the numbers of the data in the filtered LM-ICP are 358,366 and 354,247 respectively. The horizontal angle and vertical angle selected in this experiment are both 0.05°. We can see that the time cost of our proposed method in this paper can achieve about 1/1,500 of the original method, less than 1/200 of the filtered LM-ICP and almost 1/8 of NDT algorithm. In the case of registration precision, the result is better than the filtered LM-ICP, the fieltered 3D-NDT, the filtered SICP, and even the original LM-ICP. The disparities between our methods and the other methods that achieve good results are all smaller than 1mm, which is within the precision error because the experimental data are obtained from rock environment, which is enormous, and so small gap as 1mm can be neglected. Registration results are shown in Fig. 7, in which green points are points in target cloud, red points are points in source cloud and blue points are points in the transformed source point cloud. It can be seen in the figure that there is almost no difference of the registration results in visualization.

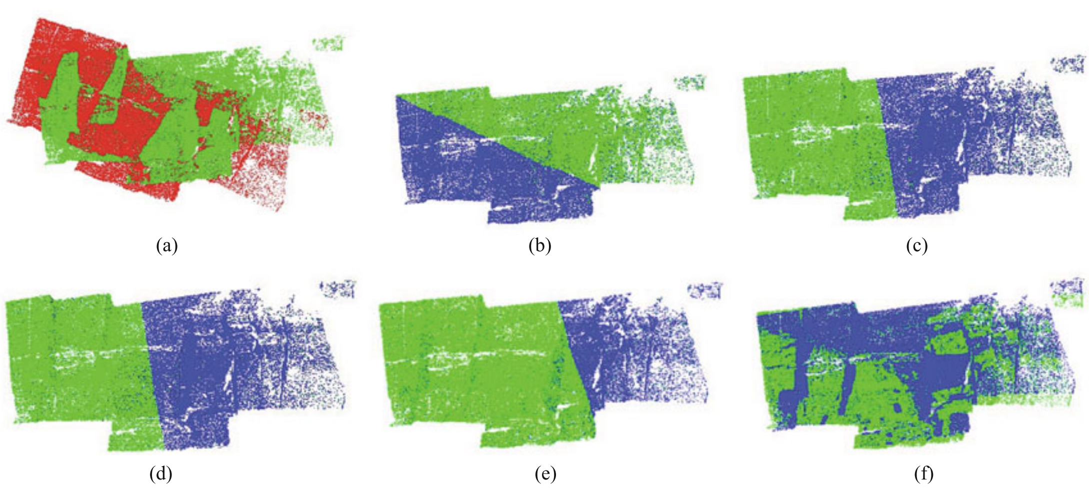

Fig. 6 Experimental results of organized point cloud. (a) Point cloud before registration which red points are source and green points are target. (b)–(f) the registration results of the proposed method, LM-ICP, filtered LM-ICP, filtered 3D-NDT and filtered SICP methods respectively, in which green points are target and blue points are the registered source

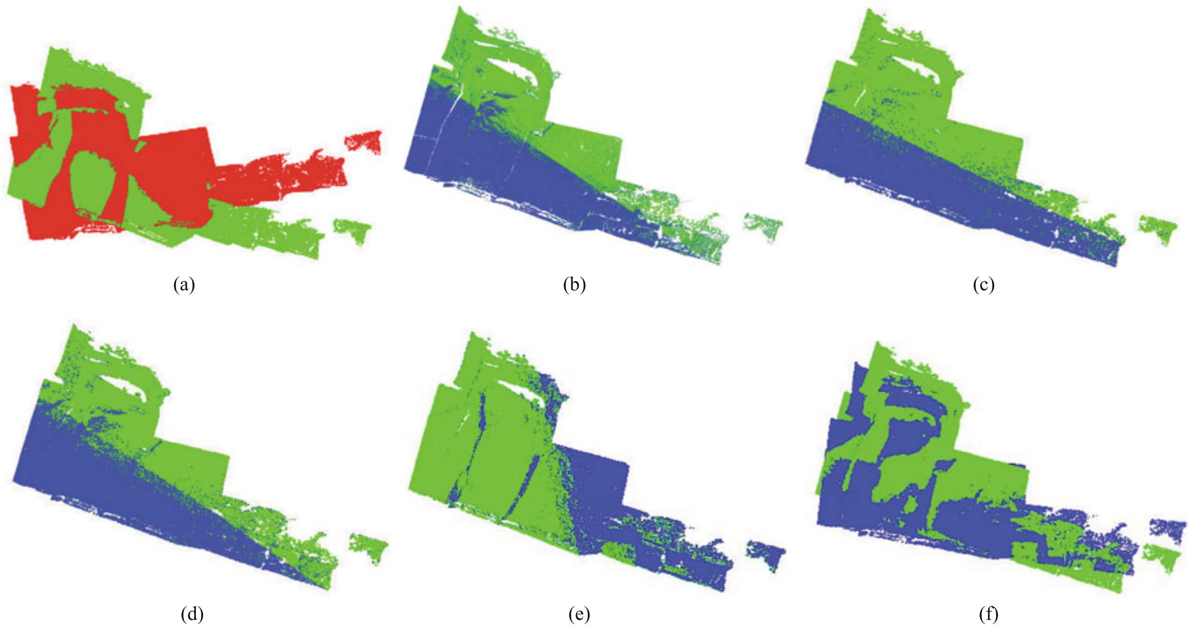

Fig. 7 Experimental results of unorganized point cloud. (a) Point cloud before registration in which red points are source and green points are target. (b)–(f) the registration results of the proposed method, LM-ICP, filtered LM-ICP, filtered 3D-NDT and filtered SICP methods respectively, in which green points are target and blue points are the registered source

Table 4 Experimental results of unorganized point cloud

Method	Time/ms	Euclidean fitness score
Proposed method	4,344	0.000966643
LM-ICP	6,570,480	0.00156585
Filtered LM-ICP	950,552	0.00210197
Filtered 3D-NDT	346,366	0.00214198
Filtered SICP	103,746,000	0.412627

In the experiments of this paper, the result of SICP is not good in both time and precision. It must be point out that the codes used in these experiments are downloaded from the website mentioned above, so there may be certain difference with the functions in PCL, and the results above are the best ones after several attempts, but may be not the best result of SICP. However, according to the experimental standard in this paper, an absolute best result will be a time-consuming process.

Figures 8 and 9 show the registration results of two clouds before and after registration. The images are the original data and the data output by computer after registration displayed by the software CloudCompare. We can see that our method can produce a good registration result for the data of considerable overlap.

5 Summary and future work

This paper presents a fast registration algorithm of rock mass point cloud based on spherical projection and feature extraction. The algorithm establishes one to one correspondence between point cloud data and pixels on the image through a spherical projection, and thus reduces the data dimension and effectively shortens the time for subsequent data process. At the same time, it utilizes the registration theory of image that is more mature developed synthetically to extract feature points in the image generated from the 2D spherical projection and search for the corresponding 3D points in the original data. Besides, we search for matching points in the

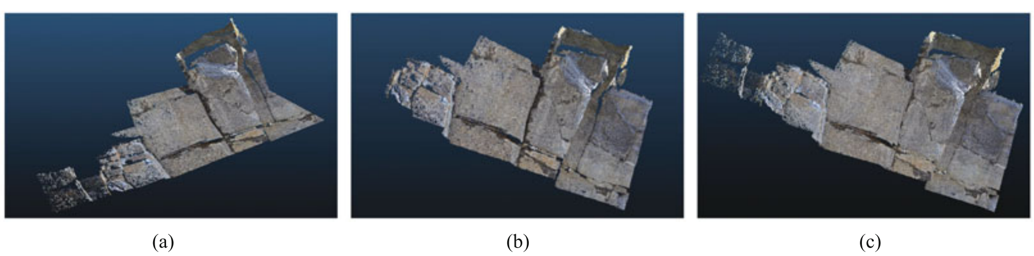

Fig. 8 Registration result of the first set of cloud. (a) Source point cloud; (b) target point cloud; (c) combination of the target and the registered source

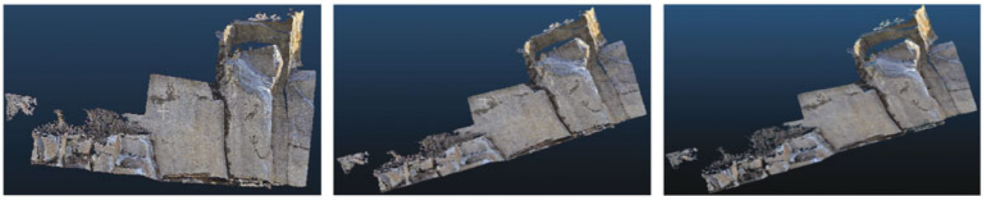

(a) (b) (c)

Fig. 9 Registration result of the second set of cloud. (a) Source point cloud; (b) target point cloud; (c) combination of the target and the registered source

two clouds and remove the false ones, then use SVD and LM-ICP to get the transformation matrix. This method reduces the amount of data used in the iteration process greatly, which not only shortens the time required for each iteration, but also reduces the number of iterations, thus significantly improves the efficiency of registration. Experimental results show that the algorithm can be applied to rock data well, and have good effects on both the organized data and the unorganized ones. In addition, it can be applied to not only the scanner data, but the non-scanner data can also get good results. The algorithm greatly improves the efficiency of registration, and has a significant advantage in dealing with massive point clouds. At present, the algorithm can achieve good result in pair-wise registration, and if a group of point clouds are imported continuously, and each of the consecutive two clouds has good initial position, then the algorithm can register them gradually and unify them to the coordinate system of the first cloud.

In the next work, we will firstly improve the steps of coarse registration and the corresponding selection, so that the correspondence between the extracted points is more accurate and more robust to non-overlapping regions, therefore to be able to get better registration result of the data that are in bad initial positions. Then we will extract public portions between source point cloud and target point cloud effectively, through which we can further reduce the computing time and get better results for data of small overlapping regions. What's more, this method can only register two sets of point clouds gradually, which may lead to an accumulation of error during the global registration. Therefore, we need to study global registration issues to get a better result of registering multi-view point cloud at the same time, while avoiding the influence of the other data in the transformation relationship of every pair of point cloud.

Acknowledgements This work was supported by the National Natural Science Foundation of China (Grant No. 61471338), Youth Innovation Promotion Association CAS (2015361), Key Research Program of Frontier Sciences, CAS (QYZDY-SSW-SYS004), Beijing Nova Program (z171100001117048), and President Fund of UCAS.

References

1. Akca D, Gruen A. A flexible mathematical model for matching of 3D surfaces and attributes. In: Proceedings of SPIE-IS&T Electronic Imaging. 2005, 184–195
2. Salvi J, Matabosch C, Fofi D, Forest J. A review of recent range image registration methods with accuracy evaluation. Image and Vision Computing, 2007, 25(5): 578–596
3. Besl P J, McKay N D. A method for registration of 3-D shapes. IEEE Transactions on Pattern Analysis and Machine Intelligence, 1992, 14(2): 239–256
4. Chen Y, Medioni G. Object modelling by registration of multiple range images. Image and Vision Computing, 1992, 10(3): 145–155
5. Farin G E, Hoschek J, Kim M S. Handbook of Computer Aided Geometric Design. Amsterdam: North-Holland, 2002
6. Wang T S, Duan Q C, Wang R. Research on registration method and precision in terrestrial 3D laser scanning. In: Proceedings of International Conference on Intelligent Earth Observing and Applications. 2015
7. Jia D F, Cheng X J, Liu Y P, Cheng X L. The orientation method of terrestrial 3D laser scanner. Geotechnical Investigation & Surveying, 2014, 10: 60–65
8. Chua C S, Jarvis R. Point signatures: a new representation for 3D object recognition. International Journal of Computer Vision, 1997, 25(1): 63–85
9. Johnson A E. Spin-Images: A Representation for 3-D Surface Matching. MPitsburgh, PA: Carnegie Mellon University, 1997
10. Stamos I, Leordean M. Automated feature-based range registration of urban scenes of large scale. In: Proceedings of IEEE Computer Society Conference on Computer Vision and Pattern Recognition. 2003, 555–561
11. Chen C, Stamos I. Semi-automatic range to range registration: a feature-based method. In: Proceedings of the 5th International Conference on 3-D Digital Imaging and Modeling. 2005, 254–261
12. Dai J L, Chen Z Y, Ye X Z. The application of icp algorithm in point cloud alignment. Journal of Image and Graphics, 2007, 12(3): 517–521
13. Manay S, Hong B W, Yezzi A J, Soatto S. Integral invariant signatures. In: Proceedings of the 8th European Conference on Computer Vision. 2004, 87–99
14. Gelfand N, Mitra N J, Guibas L J, Pottmann H. Robust global registration. In: Proceedings of the 3rd Eurographics Symposium on Geometry Processing. 2005, 197–206
15. Huang Q X, Flöry S, Gelfand N, Hofer M, Pottmann H. Reassembling

fractured objects by geometric matching. ACM Transactions on Graphics, 2006, 26(3): 569–578

16. Zhang L, Ma H C, Gao G, Chen Z. Automatic registration of urban aerial images with airborne lidar points based on line-point similarity invariants. Acta Geodaetica et Cartographica Sinica, 2014, 43(4): 372–379
17. Díez Y, Roure F, Lladó X, Salvi J. A qualitative review on 3D coarse registration methods. ACM Computing Surveys, 2015, 47(3): 45
18. Chen J, Wu X J, Wang M Y, Li X F. 3D shape modeling using a self-developed hand-held 3D laser scanner and an efficient HT-ICP point cloud registration algorithm. Optics & Laser Technology, 2013, 45(1): 414–423
19. Zhong Y, Zhang M. Automatic registration technology of point cloud based on improved ICP algorithm. Control Engineering of China, 2014, 21(1): 37–40
20. Zhao M B, He J, Luo X B, Fu Q. Two-viewing angle ladar data registration based on improved iterative closest-point algorithm. Acta Optica Sinica, 2012, 32(11): 305–314
21. Zhang L, Choi S I, Park S Y. Robust icp registration using biunique correspondence. In: Proceedings of International Conference on 3D Imaging, Modeling, Processing, Visualization and Transmission. 2011, 80–85
22. Fitzgibbon A W. Robust registration of 2D and 3D point sets. Image and Vision Computing, 2003, 21(13): 1145–1153
23. Biber P, Straβer W. The normal distributions transform: a new approach to laser scan matching. In: Proceedings of IEEE/RSJ International Conference on Intelligent Robots and Systems. 2003, 2743–2748
24. Magnusson M, Lilienthal A, Duckett T. Scan registration for autonomous mining vehicles using 3D-NDT. Journal of Field Robotics, 2007, 24(10): 803–827
25. Yang M Y, Cao Y, McDonald J. Fusion of camera images and laser scans for wide baseline 3D scene alignment in urban environments. ISPRS Journal of Photogrammetry and Remote Sensing, 2011, 66(6): S52–S61
26. Al-Manasir K, Fraser C S. Registration of terrestrial laser scanner data using imagery. The Photogrammetric Record, 2006, 21(115): 255–268
27. Łępicka M, Kornuta T, Stefańczyk M. Utilization of colour in ICP-based point cloud registration. In: Proceedings of the 9th International Conference on Computer Recognition Systems. 2016, 821–830
28. Syed I A, Sharma B. Hybrid 3D registration approach using RGB and depth images. In: Proceedings of the 2nd IEEE International Conference on Image Information Processing. 2013, 27–32
29. Lowe D G. Distinctive image features from scale-invariant keypoints. International Journal of Computer Vision, 2004, 60(2): 91–110
30. Bay H, Ess A, Tuytelaars T, Gool L V. Speeded-up robust features (SURT). Computer Vision and Image Understanding, 2008, 110(3): 346–359
31. Rublee E, Rabaud V, Konolige K, Bradski G. ORB: an efficient alternative to SIFT or SURF. In: Proceedings of International Conference on Computer Vision. 2011, 2564–2571
32. Zhang Y, Zou Z. Automatic registration method for remote sensing images based on improved orb algorithm. Remote Sensing for Land & Resources, 2013, 25(3): 20–24
33. Yang J, Cao Z, Zhang Q. A fast and robust local descriptor for 3D point cloud registration. Information Sciences, 2016, 346–347: 163–179
34. Shi P. Study on local descriptor. Shanghai: Shanghai Jiao Tong University, 2008
35. Chen C S, Hung Y P, Cheng J B. A fast automatic method for registration of partially-overlapping range images. In: Proceedings of the 6th International Conference on Computer Vision. 1998, 242–248
36. Mellado N, Aiger D, Mitra N J. Super 4PCS fast global pointcloud registration via smart indexing. Computer Graphics Forum, 2014, 33(5): 205–215
37. Perumal L. Quaternion and its application in rotation using sets of regions. International Journal of Engineering and Technology Innovation, 2011, 1(1): 35–52
38. Lato M, Kemeny J, Harrap R M, Bevan G. Rock bench: establishing a common repository and standards for assessing rockmass characteristics using lidar and photogrammetry. Computers & Geosciences, 2013, 50(1): 106–114
39. Bouaziz S, Tagliasacchi A, Pauly M. Sparse iterative closest point. Computer Graphics Forum, 2013, 32(5): 113–123

Yaru Xian received the bachelor's degree from Beihang University, China in 2013 and the master's degree from University of Chinese Academy of Sciences, China in 2016. Her research interests include computer graphics, computer vision and image processing.

Jun Xiao is now an associate professor in University of Chinese Academy of Sciences, China. He obtained his PhD degree in the Graduate University of the Chinese Academy of Sciences, China in 2008. His research interests include computer graphics, computer vision, image processing and 3D reconstruction.

Ying Wang is now a professor in University of Chinese Academy of Sciences, China. She received her PhD degree in Beijing Institute of Technology, China in 1996. Her research interests include computer graphics, visualization and computer vision.